Time of flight secondary ion mass spectrometry—A method to evaluate plasma-modified three-dimensional scaffold chemistry

Michael J. Taylor and Hannah Aitchison
NESAC/BIO, Department of Bioengineering, University of Washington, Seattle, Washington 98195

Morgan J. Hawker, Michelle N. Mann, and Ellen R. Fisher
Department of Chemistry, Colorado State University, Fort Collins, Colorado 80523-1872

Daniel. J. Graham and Lara. J. Gamble[a)]
NESAC/BIO, Department of Bioengineering, University of Washington, Seattle, Washington 98195

(Received 19 January 2018; accepted 19 March 2018; published 30 March 2018)

Biopolymers are used extensively in the manufacture of porous scaffolds for a variety of biological applications. The surfaces of these scaffolds are often modified to encourage specific interactions such as surface modification of scaffolds to prevent fouling or to promote a cell supportive environment for tissue engineering implants. However, few techniques can effectively characterize the uniformity of surface modifications in a porous scaffold. By filling the scaffold pores through polymer embedding, followed by analysis with imaging time-of-flight secondary ion mass spectrometry (ToF-SIMS), the distribution and composition of surface chemical species though complex porous scaffolds can be characterized. This method is demonstrated on poly(caprolactone) scaffolds modified with a low-fouling plasma-deposited coating from octafluoropropane via plasma enhanced chemical vapor deposition. A gradient distribution of CF^+/CF_3^+ is observed for scaffolds plasma treated for 5 min, whereas a 20 min treatment results in more uniform distribution of the surface modification throughout the entire scaffold. The authors expect this approach to be widely applicable for ToF-SIMS analysis of scaffolds modified by multiple plasma processing techniques as well as alternative surface modification approaches.
Published by the AVS. https://doi.org/10.1116/1.5023005

I. INTRODUCTION

Examples of surface chemical modifications of biopolymers are widespread in a variety of applications, from tissue engineering[1] to manufacture of stents[2] and catheters.[3]

Surface characterization techniques such as time-of-flight secondary ion mass spectrometry (ToF-SIMS) and x-ray photoelectron spectroscopy (XPS) have been successful at characterizing surface modification of many types of 2D (flat) surfaces.[4–7] Flat surfaces are, however, rarely utilized in biomaterial applications.

Instead, three-dimensional structures such as porous scaffolds are more suited for applications such as biofilters or in tissue engineering. The pores, or channels, of the scaffolds allow for mass-transport which is vital for cell nutrition and migration, as well as mimic the extracellular matrix[8] providing surface features for cell attachment.[9] Unfortunately, modification of complex multisurface scaffolds may result in variable distribution of surface presenting moieties.[10] Relatively few techniques are effectively used to characterize the chemical uniformity of surface modification throughout topographically complex substrates. Techniques such as XPS (Ref. 11) and ToF-SIMS (Ref. 12) have been shown to be ideally suited in determining the surface chemical composition of synthetic[13,14] and biologically manufactured materials[15,16] with detection limits below 10 ng/cm^2 for adsorbed proteins on polymeric substrates.[17] The structure of porous materials, however, presents a number of challenges for these surface sensitive techniques. Unfortunately, XPS lacks the high spatial resolution required for imaging sub-15 μm scaffold fibers,[18] whereas ToF-SIMS studies have involved harsh methods of pore filling[19] to reduce surface topography which may damage and warp softer, flexible scaffolds such as those produced from poly(caprolactone) (PCL). An improved method to qualify the distribution of surface modifications throughout topographically complex samples such as polymer scaffolds would greatly aid our ability to correlate surface chemical modifications to scaffold performances.

Lateral spatial resolutions of <1 μm are attainable with ToF-SIMS, allowing discrete changes in distribution of chemical species on multilayer materials to be mapped. Although ToF-SIMS may seem ideal for characterizing the modification of scaffold surfaces, the quality of data, unfortunately, is strongly dependent on the morphology of the substrate. Surface topography on the order of microns can result in lateral distortion in imaged secondary ions or shadowing in the image.[20,21] An extraction delay postrastering of the ion beam may circumvent some of these topographic effects.

Porous scaffolds, however, may have changes in topography of >1 μm, which can be problematic for ToF-SIMS analysis, depending on the instrument configuration, even when using these methods. To effectively map chemical species in the coated, organic scaffolds, we have utilized a milder method of pore filling to embed the scaffolds

[a)]Electronic mail: lgamble@uw.edu

with polyvinyl alcohol (PVA), followed by freezing and cryo-sectioning cross-sections of the scaffolds. Using this method, surface sensitive techniques such as ToF-SIMS and XPS can be used to provide a detailed understanding of the distribution and composition of surface chemical species in surface modified scaffolds. Embedding topographic scaffolds in a polymer prior to analysis not only minimizes topographical effects but also provides structural support, allowing sequential cross-sections of the scaffold to be prepared.

Here, we demonstrate the utility of this method by characterizing fluorocarbon (FC) films deposited throughout PCL scaffolds using octofluoropropane (C_3F_8) plasma enhanced chemical vapor deposition (PECVD). PECVD is a versatile tool to produce modified surfaces via film deposition or grafting of reactive groups[22–25] which Hawker *et al.* have previously demonstrated through modification of PCL scaffolds by PECVD using C_3F_8.[22] We use PVA embedding and cross-sectioning sample preparation followed by ToF-SIMS imaging to map the distribution of FC plasma treatment of PCL scaffolds modified by PECVD demonstrating that a longer treatment time deposits a more uniform coating throughout the scaffold whilst a shorter treatment deposits a gradient distribution of FC.[26]

II. EXPERIMENT

A. Scaffold fabrication and modification

PCL scaffolds prepared via porogen leaching methods were fabricated and plasma treated with C_3F_8 as previously reported.[22] Briefly, scaffolds were prepared by dissolving PCL pellets (average $M_n = 80\,000$) in chloroform. As-received sodium chloride was seived, and NaCl crystals (150–300 μm) were added to the dissolved PCL/chloroform mixture in a 5:95 w/w ratio of PCL:NaCl. The mixture was cast into Teflon molds, dried, and immersed in deionized water (DI) water for several days. After removing scaffolds from molds and drying under ambient conditions, scaffolds were modified by PECVD in a home-built, glass barrel style plasma reactor, inductively coupled to the C_3F_8 feedgas (Airgas, 99.96% purity) using a Ni-plated copper coil. Precursor gas flow rate was controlled at 5 sccm (corresponding to a total reactor pressure of 50 mTorr) using a MKS mass flow controller, and pressure was monitored using a Baratron capacitance manometer. Typically, six scaffolds were treated at a time, placed on a clean glass slide 15 cm downstream from the coil region. The plasma was generated at 50 W using a radio frequency (13.56 MHz) power supply applied through a matching network. Plasma treatment times were 5 and 20 min.

B. Scaffold embedding and slicing

The plasma-treated scaffold disks were initially sectioned in half horizontally by hand to expose the interior face using a disposable microtome blade (Accu-Edge Low Profile 4689). This manually cut scaffold half was then immersed in PVA (Sigma Aldrich) (12% w/v) in DI (>18 MΩ cm) water. Prior to scaffold immersion, the PVA was purified by dialysis ten times to remove salt, similar to the procedure described in the literature.[27] The scaffold was gently depressed on all sides while submerged using tweezers until the absence of air bubbles was observed. After 72 h immersion, the scaffold half was removed and submerged in fresh PVA solution, followed by freezing in dry ice for 60 min. Then, the PVA embedded scaffold half was mounted on a stub to expose the frozen lateral face of the scaffold and sectioned using a Leica CM1580 cryostat at −20 °C with a section thickness of 30 μm. The scaffold slices were mounted on 1×1 cm^2 silicon wafers prior to loading onto the top-mount stage or sample bar for ToF-SIMS and XPS analysis, respectively. A schematic representation of this procedure is shown in supplementary material, Fig. 1.[32]

C. Instrumentation

ToF-SIMS analysis was performed on an ION-ToF TOF-SIMS 5 (IONTOF GmbH, Münster, Germany) instrument using a Bi_3^+ liquid metal ion gun in delayed extraction mode with an energy of 25 keV. For each rectangular section of the PCL scaffold, a line profile was analyzed, comprising 8–10 analysis areas (500×500 μm). The result was a 0.5×4–5 mm strip covering the short length of the section, from the top face of the scaffold to the bottom. The target current of the

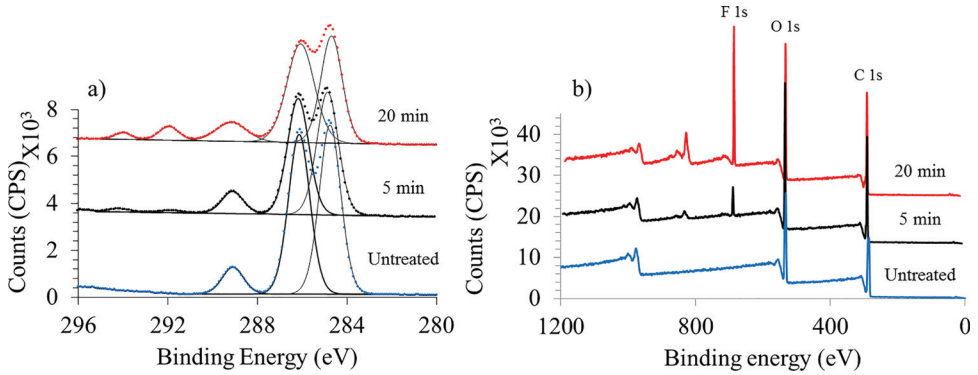

FIG. 1. XPS C1s high resolution spectra (a) and survey spectra (b) corresponding to C_3F_8 plasma treated PCL scaffold from analysis of scaffold cross-section. Untreated (blue, bottom), 5 min (black, middle), and 20 min (red, top). Three (300×700 μm) spots from each treatment time were taken from three replicates. Spectra are stacked for clarity in Y axis.

analysis beam was set to 0.11 pA. Each $500 \times 500\,\mu$m area was rastered in a random pattern across 256×256 pixels. The ion dose was 1.80×10^{10} ions cm^{-2}, ensuring the measurements were made under static SIMS conditions. An electron flood gun was used to neutralize any charge build up. Data processing was performed using SURFACELAB 6 (IONTOF GmbH, Münster, Germany). Positive ion spectra were collected over the mass range of m/z 0–800. Three separate slices from the same scaffold were imaged, with three line scans measured per section, yielding 9 line scan measurements in total. Normalization of line scans was done by dividing the summed intensity of the given peaks for the pixels in a given line, by the total intensity of the pixels in the same line. Mass resolution of the $C_2H_3^+$ secondary ion (m/z 27) was above 2000. The spectra were mass calibrated using the CH_3^+, $C_2H_3^+$, and $C_3H_5^+$ peaks.

XPS analysis of the scaffold sections was performed on a Kratos AXIS Ultra DLD instrument featuring a monochromated Al K_α x-ray source operated at 150 W with a pass energy of 80 eV for composition analysis and 20 eV pass energy for high resolution C_{1s} scans using the slot mode. Charge neutralization was used and three different spots were analyzed on three different samples for a total of nine spots per sample type.

The data were processed with CASA XPS (v2.3.12) using empirically derived sensitivity factors. Wide scan and high resolution C_{1s} spectra were calibrated to the hydrocarbon peak at (285.0 eV). Peak fitting was performed using five components: aliphatic (C-C/C-H) (285.0 eV), alcohol/ether (C-O-R) (286.2 eV), ester (O-C=O) (288.7), and fluoroalkyl (C-F_2/C-F_3) (291.6/293.7 eV) bonding. The full width half maximum was set at 1.13 eV for C_{1s} components with fixed peak positions at the binding energies stated using Gaussian function leaving only the peak intensities to vary with peak fit.

III. RESULTS

The aim of this study was to develop a method to assess the distribution of FC species in PECVD treated scaffolds across the entire scaffold body, thereby identifying any differences in deposition behavior throughout the 3D scaffold. This method involves embedding the PCL scaffold disks in PVA which allows filling of the construct pores, cryosectioning the samples, and mounting them on Si wafers for ToF-SIMS and XPS analysis (supplementary material, Fig. 1). The PVA was dialyzed before embedding the scaffold to reduce the amount of salt present. We found that three days was sufficient to allow for the ingression of PVA into the pores, and produced mostly pore-filled slices with no observed evidence of scaffold tearing through sectioning or mounting on the silicon wafer substrate.

XPS surface chemical analysis of a PVA control and the PVA embedded scaffolds are shown in Table I and example spectra of the PVA embedded scaffolds are depicted in Fig. 1. No fluorine was detected by XPS in the untreated scaffold whereas significant levels of fluorine are found in both the 5 and 20 min plasma treated scaffolds.

TABLE I. Elemental and component contributions to C_{1s} peak from cross-sections. n/d = not detected (<0.1%).

	XPS (at. %)			
Scaffold	C	O	F	Si
PVA	65.4 ± 0.2	34.6 ± 0.1	n/d	n/d
Untreated	72.5 ± 0.6	27.5 ± 0.4	n/d	n/d
5 min C_3F_8	67.1 ± 1.7	25.3 ± 0.5	7.7 ± 4.1	0.1 ± 0.0[a]
20 min C_3F_8	60.6 ± 4.0	14.9 ± 2.1	24.3 ± 2.1	n/d

	Component contributions to C_{1s} peak (%)				
Scaffold	C-C/C-H	C-O-R	O-C-O	C-F_2	C-F_3
PVA	49.5 ± 0.2	50.5 ± 0.1	n/d	n/d	n/d
Untreated	45.0 ± 0.8	48.9 ± 0.7	6.1 ± 1.1	n/d	n/d
5 min C_3F_8	46.5 ± 1.3	44.1 ± 1.6	8.3 ± 0.1	1.0 ± 0.3	0.8 ± 0.1
20 min C_3F_8	38.2 ± 3.5	44.6 ± 2.3	10.1 ± 1.3	4.6 ± 0.7	2.6 ± 0.6

[a]Detected in 1 of 3 spots analyzed.

This is in agreement with previously published data by Hawker *et al.*[26] that showed increase in F content with increase in deposition time. Unsurprisingly, scaffolds treated for the longer time (20 min) contained more FC species throughout the scaffold than those treated for shorter time (5 min). The decrease in the standard deviation of the amount of fluorine from 5 to 20 min treatment in these measurements indicates that the fluorine distribution is more homogeneous across the cross-section after the longer treatment time.

The percentage of carbon measured decreases as a function of scaffold treatment time owing to a higher ratio of fluorine present in the C_3F_8 plasma precursor as compared to carbon. Additionally, oxygen content decreases in the treated samples as the FC film layer attenuates signal from the underlying PCL. A small amount of silicon was detected in XPS analysis of the PVA embedded scaffolds in one of the samples. No poly(dimethyl siloxane) was detected in SIMS analysis of this sample suggesting that presence of silicon was related to the scaffold filling or tearing during sectioning rather than external contamination.

The C_{1s} high resolution spectra of the PCL untreated scaffold [Fig. 1(a)] was fit with three components: C-C (285.0 eV), C-O-C (286.2 eV), and O-C=O (288.7 eV).

Peak fit areas are reported in Table I. C_3F_8 plasma treatment results in additional contributions at ~290.9 and 292.7 eV, corresponding to CF_2 and CF_3. The peak contributions from each of the FC components increase from the 5 to the 20 min samples by 3.6% and 1.8% for the CF_2 and CF_3 species, respectively (Table I). This is consistent with an increase in CF_2 and CF_3 in a 2:1 ratio as expected for deposition from the C_3F_8 monomer. Contributions from the underlying PCL-related components also decrease for longer treatment times, further supporting the observation that FC coverage of the PCL scaffold increases with treatment time.

Normalized ToF-SIMS spectra of the C_3F_8 plasma-treated scaffold cross-sections (embedded in PVA) are

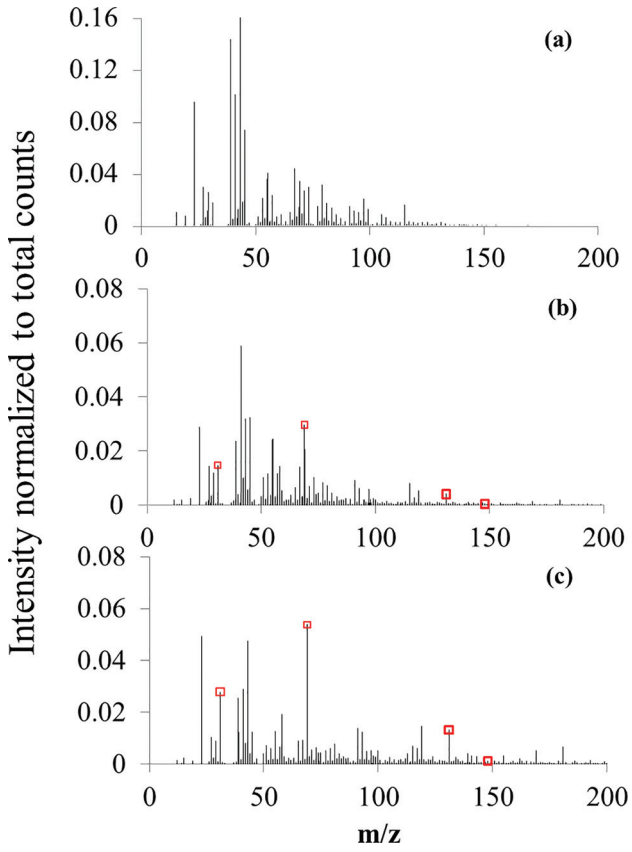

FIG. 2. Positive ion spectra acquired from (500 × 4000 μm) cross-sections of (a) untreated PCL scaffolds, (b) 5 min and (c) 20 min C_3F_8 plasma-treated PCL scaffolds. Electropositive peaks CF^+ (*m/z* 31.01) CF_3^+ (*m/z* 68.99), $C_3F_5^+$ (*m/z* 130.99), and $C_3F_6^+$ (149.99) are highlighted with red boxes.

shown in Fig. 2 for the mass range of 0–200 m/z. Peaks detected at 31, 69, 131, 150, 169 and 593 *m/z* were identified as CF^+, CF_3^+, $C_3F_5^+$, $C_3F_6^+$, $C_3F_7^+$ and an adduct $C_{13}F_{23}^+$, respectively. A tenfold increase in FC intensity was observed from imaging the embedded 5 min treated cross-section, compared to the unembedded scaffold which is shown in supplementary material, Fig. 3. Normalized peak intensities of CF^+, CF_3^+, $C_3F_5^+$ and $C_3F_6^+$ are indicated by squares in the spectra in Fig. 2.

These fluorocarbon peaks increase from background counts in the untreated PCL scaffold to 0.012 and 0.032 normalized counts, respectively, for the 5 min treated sample, and 0.018 and 0.047 for the 20 min treated sample. These results are consistent with the XPS results indicating that more organofluorine is deposited in the scaffold interior after longer treatment. PCL and PVA-related peaks (e.g., C_xH_yO species) were also identified as well as sodium. The contribution of sodium to the total ion intensity of the spectra of all samples analyzed was <8%, indicating matrix effects were likely insignificant.[28] Peak assignments are summarized in supplementary material Table I. No significant peaks corresponding to FC fragments were observed on the untreated scaffolds or PVA control.

ToF-SIMS imaging was used to map the changes in lateral distribution of the FC coating across the scaffold (Fig. 3) showing the sum of key FC ions and $C_6H_9O_2^+$ (representative

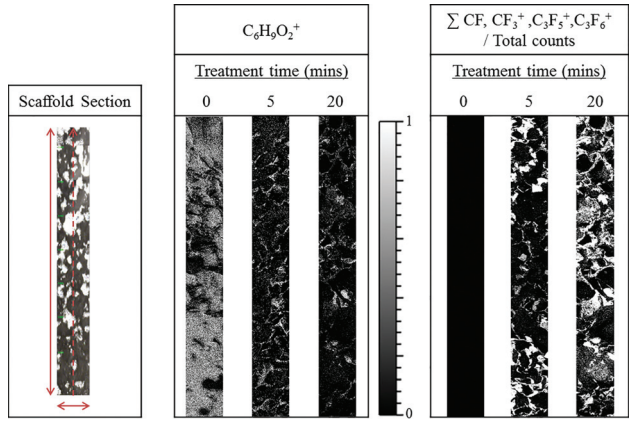

FIG. 3. Image in the first column is a representative photomicrograph of an unmodified PCL scaffold, the direction of analysis for the corresponding secondary ion images is detailed by the red dashed line (500 × 4000 μm). The second and third columns are ToF-SIMS image area scans (500 × 4000 μm) from cross-sections of C_3F_8 plasma treated (0, 5, and 20 min) PCL scaffolds following the $C_6H_9O_2^+$ ion (PCL substrate) and a sum of FC ions from the plasma deposition film.

of PCL scaffold). Imaging of the scaffold fiber prior and following embed is shown in supplementary material, Fig. 2. The FC overlayer and scaffold fibers are clearly shown in the red/green/blue overlayer using PVA embedding. The summed intensities normalized to total for CF^+, CF_3^+, $C_3F_5^+$, and $C_3F_6^+$ were used to determine surface treatment distribution. These peaks were chosen because they have the largest relative intensities compared to other fluorine containing secondary ions. A photomicrograph of a 30 μm thin scaffold section (5 min C_3F_8 deposition) in Fig. 3 details the structure of the embedded scaffold, with the darker regions corresponding to PCL, whereas the lighter regions correspond to PVA. From the summed FC ToF-SIMS images, we see that for the 5 min treated sample, the image is brighter toward the ends of the image, indicating the fluorocarbon was predominantly deposited at the outer edges of the scaffold.

In contrast, a more uniform distribution of FC is observed in the image for the 20 min treated sample.

The scale bar shown represents the normalized to total intensity of secondary ions ($C_6H_9O_2^+$) or summed normalized to total FC secondary ions (CF^+, CF_3^+, $C_3F_5^+$, and $C_3F_6^+$).

The normalized intensity of CF^+ and CF_3^+ through the cross-sections of the control and treated scaffolds (line scans—Fig. 4) were used to compare the distribution of signals between the two different deposition times. The untreated PCL scaffold plot provides a control measurement as no FC signals are observed for these materials. This also provides a basis to observe the trend in CF^+ and CF_3^+ distribution.

The scans for scaffolds treated for 5 min display a gradient distribution, with a higher intensity of CF^+ and CF_3^+ in the first 0–1 mm and last 3–4 mm of the scan, whereas a lowered intensity is observed in the middle 1–3 mm. In contrast, the image of scaffolds treated for 20 min does not show a gradient trend in CF^+ and CF_3^+ distribution.

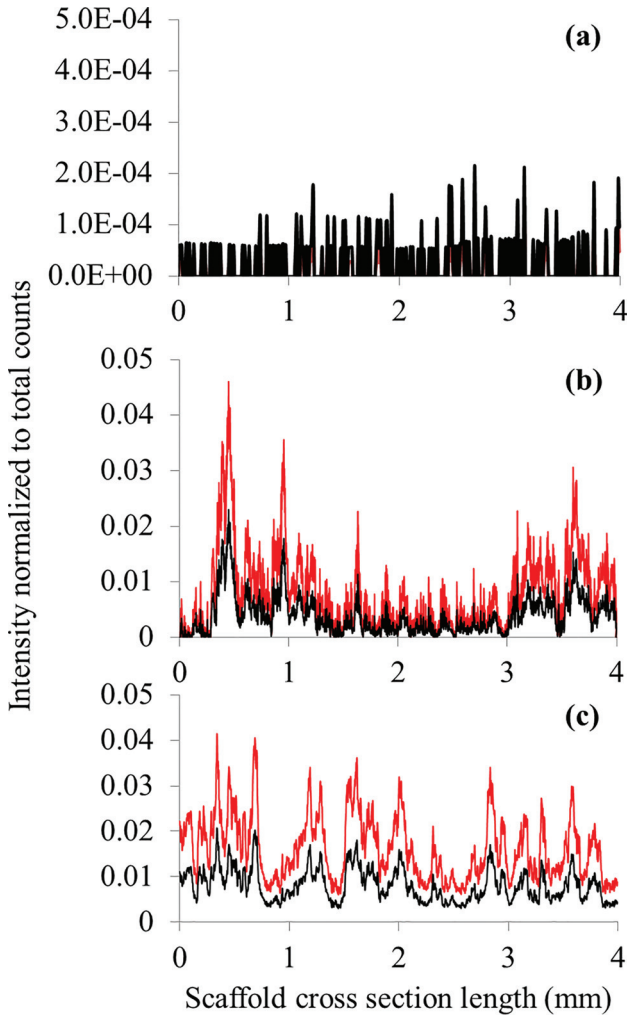

FIG. 4. ToF-SIMS line scans of CF^+ (black) and CF_3^+ (red) intensity, respectively, from cross-sections from C_3F_8 plasma-treated PCL scaffold. Singular line scans from (a) untreated, (b) 5 min and (c) 20 min plasma treatment.

IV. DISCUSSION

Here, we have developed a method for filling PCL porous scaffolds with PVA and analyzing with XPS and imaging ToF-SIMS to assess the distribution of fluorocarbon coatings deposited on the scaffolds. Dialysis of the PVA prior to embedment was necessary to reduce the potential matrix effects of salts such as secondary ion ionization suppression which may mask FC related secondary ion intensities.

A three-day immersion of the PCL scaffold disks in PVA was required to fully fill pores. This relatively low rate of PVA ingression into the scaffold pores was likely due to the inherent hydrophobicity of PCL, resisting water absorption into the scaffold core.[29]

Although the PVA embedding material changed the relative elemental composition detected by XPS, fluorine deposited by the plasma was still detected in the PCL scaffold cross-sections. As compared to XPS data previously published by Hawker *et al.*,[26] a lower atomic percentage of fluorine was detected. This result is not surprising as the embedding material not only contributed additional carbon and oxygen to the overall atomic composition, but it also likely attenuated signal from the FC coating in some regions of the scaffold. A comparison of XPS atomic compositions of the PVA embedded FC modified scaffolds with the PVA embedded control scaffold reveals an increase in fluorine with increasing FC deposition time. This increase in fluorine is concomitant with a decrease in oxygen and carbon, consistent with attenuation of the scaffold substrate signal. These XPS trends are consistent with previous data.[26]

ToF-SIMS images of the scaffold cross-sections were used to determine the distribution of FC deposition in the samples. The gradient distribution observed in the 5 min treated sample (Fig. 4) showed most of the fluorocarbon intensity at the edges of the scaffold and indicated that at shorter deposition times the plasma does not deposit throughout the interior of the scaffold. The distributions on the scaffold treated for 20 min, however, indicated that there was a more uniform scaffold coating with FC deposition internally as well as externally. If the FC plasma species had a higher sticking coefficient to the "as deposited" FC coating on the scaffold exterior than the unmodified scaffold areas in the interior, the longer deposition times would likely manifest as a gradient of higher FC at the exterior of the scaffold than the interior. Our results, however, indicate an even deposition throughout the scaffold for increased treatment time, indicating that the plasma had higher sticking probability to the scaffold substrate than to the FC film. Studies have reported diffusion to be a controlling factor in the deposition of plasma species in 3D scaffolds[11,30,31] which is consistent with our results that indicate initial deposition of the FC polymer is likely diffusion limited. Hawker *et al.* demonstrated the non-self-limiting behavior of FC films on flat steel substrates via ellipsometry,[26] indicating the FC film may continue to be deposited on FC modified substrate, but likely with a lower rate than the initial deposition on the PCL scaffold substrate.

V. SUMMARY AND CONCLUSIONS

We have demonstrated that the method of embedding and sectioning followed by ToF-SIMS surface characterization of PECVD modified PCL scaffolds can be used to readily map the chemical distribution of surface modification in morphologically challenging porous materials. Specifically, embedding PCL scaffolds in PVA followed by sectioning produces samples appropriate for mapping FC distribution with imaging ToF-SIMS. These results indicate apparent differences in the FC deposition distribution between the 5 and 20 min treatment times. ToF-SIMS line scans following the FC deposition showed more FC deposition at the scaffold edges on the 5 min sample, whereas the 20 min sample had more even distribution of the plasma film, indicating that the deposition process was likely diffusion limited. These data demonstrate that ToF-SIMS characterization holds significant promise for determining conformality of coatings/modifications in complex three-dimensional samples. Such knowledge of coating uniformity and composition can guide

fabrication and surface modification of materials with complex geometries.

ACKNOWLEDGMENTS

The authors would like to thank the NIH for funding this work (No. NESACBIO NIH P41 EB002027), as well as G. Hammer and W. Cridion for their expertise in XPS and sample preparation, respectively. E.R.F. acknowledges financial support from the National Science Foundation (No. NSF-1152963).

[1]N. U. Tirelli, M. P. Lutolf, A. Napoli, and J. A. Hubbell, Mol. Biotechnol. **90**, 3 (2002).
[2]A. Strohbach and R. Busch, Int. J. Polym. Sci. **2015**, 782653.
[3]J. D. Bryers, Biotechnol. Bioeng. **100**, 1 (2008).
[4]D. G. Castner and B. D. Ratner, Surf. Sci. **500**, 28 (2002).
[5]P. Kingshott, G. Andersson, S. L. McArthur, and H. J. Griesser, Curr. Opin. Chem. Biol. **15**, 667 (2011).
[6]N. Médard, M. Aouinti, F. Poncin-Epaillard, and P. Bertrand, Surf. Interface Anal. **31**, 1042 (2001).
[7]C. Y. Lee, G. M. Harbers, D. W. Grainger, L. J. Gamble, and D. G. Castner, J. Am. Chem. Soc **129**, 9429 (2007).
[8]L. Freed, G. Vunjak-Novakovic, R. Biron, D. Lesnoy, S. Barlow, and R. Langer, Nat. Biotechnol. **2**, 689 (1994).
[9]L. R. Madden *et al.*, Proc. Natl. Acad. Sci. **107**, 15211 (2010).
[10]X. Liu, Y. Won, and P. X. Ma, J. Biomed. Mater. Res., Part A **74**, 84 (2005).
[11]J. J. A. Barry, M. M. C. G. Silva, K. M. Shakesheff, S. M. Howdle, and M. R. Alexander, Adv. Funct. Mater. **15**, 1134 (2005).
[12]C. Sarra-Bournet, S. Poulin, K. Piyakis, S. Turgeona, and G. Larochea, Surf. Interface Anal. **42**, 102 (2010).
[13]C. A. Barnes, J. Brison, R. Michel, B. N. Brown, G. David, S. F. Badylak, B. D. Ratner, and W. Engineered, Biomaterials **32**, 137 (2011).
[14]M. Taylor, D. Scurr, M. Lutolf, L. Buttery, M. Zelzer, and M. Alexander, Biointerphases **11**, 02A301 (2016).
[15]L. A. Klerk, P. Y. W. Dankers, E. R. Popa, A. W. Bosman, M. E. Sanders, K. A. Reedquist, and R. M. A. Heeren, Anal. Chem. **82**, 4337 (2010).
[16]H. E. Canavan, D. J. Graham, X. Cheng, B. D. Ratner, and D. G. Castner, Langmuir **23**, 50 (2007).
[17]M. S. Wagner, S. L. McArthur, M. Shen, T. A. Horbett, and D. G. Castner, J. Biomater. Sci. Polym. Ed. **13**, 407 (2002).
[18]C. J. Blomfield, J. Electron Spectrosc. Relat. Phenom. **143**, 241 (2005).
[19]D. Wang, G. Poologasundarampillai, W. van den Bergh, R. J. Chater, T. Kasuga, J. R. Jones, and D. S. McPhail, Biomed. Mater. **9**, 15013 (2014).
[20]S. Koch, G. Ziegler, and H. Hutter, Anal. Bioanal. Chem. **405**, 7161 (2013).
[21]S. Rangarajan and B. J. Tyler, J. Vac. Sci. Technol. **24**, 1730 (2006).
[22]P. Favia and R. d'Agostino, Surf. Coat. Technol. **98**, 1102 (1998).
[23]M. Vasudev, P. Anderson, T. Bunning, V. Tsukruk, and R. Rajesh, ACS Appl. Mater. Interfaces. **10**, 3983 (2013).
[24]J. H. Yim, M. S. Fleischman, V. Rodriguez-Santiago, L. T. Piehler, A. A. Williams, J. L. Leadore, and D. D. Pappas, ACS Appl. Mater. Interfaces **5**, 11836 (2013).
[25]F. R. Marciano, D. A. Lima-Oliveira, N. S. Da-Silva, E. J. Corat, and V. J. Trava-Airoldi, Surf. Coat. Technol. **204**, 2986 (2010).
[26]M. J. Hawker, A. Pegalajar-Jurado, and E. R. Fisher, Langmuir **30**, 12328 (2014).
[27]M. Egginger, M. Irimia-Vladu, R. Schwodiauer, A. Tanda, S. Bauer, and S. Sariciftici, Adv. Mater. **20**, 1018 (2008).
[28]R. Garret, R. Macdonald, and D. O'conner, Nucl. Instrum. Methods Phys. Res. **218**, 333 (1983).
[29]S. T. Yohe, J. D. Freedman, E. J. Falde, Y. L. Colson, and M. W. Grinstaff, Adv. Funct. Mater. **23**, 3628 (2013).
[30]J. W. Bradley, B. Abdullah, and M. R. Alexander, "Using plasma discharges to chemically functionalise 3-D tissue engineering scaffolds," in *17th International Conference on Gas Discharges and their Applications* (2008), pp. 497–499.
[31]A. J. Beck, F. R. Jones, and R. D. Short, Polymer **37**, 5537 (1996).
[32]See supplementary material at https://doi.org/10.1116/1.5023005 for additional information and data.